Cell

RNA Clamping by Vasa Assembles a piRNA Amplifier Complex on Transposon Transcripts

Jordi Xiol,[1,2,7] Pietro Spinelli,[1,2] Maike A. Laussmann,[1,2,3] David Homolka,[1,2] Zhaolin Yang,[1,2] Elisa Cora,[1,2] Yohann Couté,[4] Simon Conn,[1,2] Jan Kadlec,[1,2] Ravi Sachidanandam,[5] Marko Kaksonen,[3] Stephen Cusack,[1,2] Anne Ephrussi,[6] and Ramesh S. Pillai[1,2,*]

[1]European Molecular Biology Laboratory, Grenoble Outstation
[2]Unit for Virus Host-Cell Interactions
University Grenoble Alpes-EMBL-CNRS, 71 avenue des Martyrs, 38042, France
[3]Cell Biology and Biophysics Unit, EMBL, 69117 Heidelberg, Germany
[4]Laboratoire Biologie à Grande Echelle, IRTSV, CEA, 38054 Grenoble, France
[5]Department of Oncological Sciences, Icahn School of Medicine at Sinai, New York, NY 10029, USA
[6]Developmental Biology Unit, EMBL, 69117 Heidelberg, Germany
[7]Present address: Department of Cell Biology, Harvard Medical School, Boston, MA 02115, USA
*Correspondence: pillai@embl.fr
http://dx.doi.org/10.1016/j.cell.2014.05.018

SUMMARY

Germline-specific Piwi-interacting RNAs (piRNAs) protect animal genomes against transposons and are essential for fertility. piRNAs targeting active transposons are amplified by the ping-pong cycle, which couples Piwi endonucleolytic slicing of target RNAs to biogenesis of new piRNAs. Here, we describe the identification of a transient Amplifier complex that mediates biogenesis of secondary piRNAs in insect cells. Amplifier is nucleated by the DEAD box RNA helicase Vasa and contains the two Piwi proteins participating in the ping-pong loop, the Tudor protein Qin/Kumo and antisense piRNA guides. These components assemble on the surface of Vasa's helicase domain, which functions as an RNA clamp to anchor Amplifier onto transposon transcripts. We show that ATP-dependent RNP remodeling by Vasa facilitates transfer of 5′ sliced piRNA precursors between ping-pong partners, and loss of this activity causes sterility in *Drosophila*. Our results reveal the molecular basis for the small RNA amplification that confers adaptive immunity against transposons.

INTRODUCTION

Mobile genomic elements called transposons constitute a large part of eukaryotic genomes and present a formidable threat to genome integrity due to their ability to cause mutations or ectopic recombination events (Kazazian, 2004). Animal gonads employ the dedicated PIWI clade Argonautes and their associated 24–30 nucleotide (nt) Piwi-interacting RNAs (piRNAs) to suppress transposon activity. piRNAs guide Piwi proteins to their transposon targets, which are identified by sequence complementarity between the piRNA and the target. Some Piwi proteins function as small RNA-guided endoribonucleases (slicers), whereas nuclear Piwi complexes may also mediate silencing by altering chromatin or DNA methylation status of target genomic loci. The importance of this pathway is highlighted by the fact that Piwi mutants display infertility due to defects in germline development, presumably as a result of genome instability caused by transposon activation (Bagijn et al., 2012; Ghildiyal and Zamore, 2009; Luteijn and Ketting, 2013).

Guidance information for Piwi proteins is genetically encoded into a few hundred genomic regions called piRNA clusters (Brennecke et al., 2007). These genomic intervals serve as a registry of all transposons hosted in the genome by containing a high density of transposon fragment insertions. Clusters are transcribed into a long single-stranded piRNA precursor (up to 100 kb long) and are then exported to the cytoplasm by RNA export factors like Uap56 (Zhang et al., 2012) for maturation into tens of thousands of piRNAs via a poorly understood primary processing pathway (Brennecke et al., 2007). Processing is believed to take place in cytoplasmic perinuclear granules called nuage that concentrate most known piRNA processing factors (Lim and Kai, 2007). By providing germ cells with a complex mixture of sequences to target all mobile elements present in the genome, these primary piRNAs act as the genetically encoded component of an RNA-based innate immune system (Aravin et al., 2007).

Germ cells have an additional and more elegant piRNA biogenesis pathway where target silencing itself triggers generation of new piRNAs. Sequence analyses of small RNAs associating with the *Drosophila* Piwi proteins (Aubergine and Ago3) formed the basis for such a proposal, and these ideas are incorporated into the so-called ping-pong model (Brennecke et al., 2007; Gunawardane et al., 2007). It is proposed that antisense primary piRNAs guide Aubergine (Aub) for cytoplasmic endonucleolytic

cleavage (slicing) of target transposon RNAs. One of the resulting cleavage fragments is then utilized to generate a new secondary piRNA that associates with Ago3, with the cleavage site marking its 5′ end. Given their origin from transposon transcripts, Ago3-bound piRNAs are of sense orientation. These, in turn, guide Ago3 slicer activity to complementary cluster transcripts, with a cleavage fragment maturing exactly as the same Aub-bound antisense piRNA that initiated the transposon cleavage. In such a scenario, Ago3 slicing serves to prioritize production of specific antisense piRNAs from piRNA cluster transcripts (Li et al., 2009). The system is built such that abundant transposons will produce more Ago3-loaded piRNAs, resulting in even greater production of antisense piRNAs in Aub. Such a feedforward amplification loop represents the adaptive arm of the RNA-based immune system that monitors transposon activity and selectively amplifies those piRNAs that target the most active transposons. The versatility of the ping-pong cycle is evident from the fact that maternally deposited piRNAs can also serve as inputs, thereby allowing the embryo to rapidly ramp up immunity against paternally inherited transposons to avert infertility caused by hybrid dysgenesis (Brennecke et al., 2008; Grentzinger et al., 2012). It can also promote emergence of new piRNA loci by targeting genomic regions in *trans* (de Vanssay et al., 2012).

We currently do not understand how such a complex small RNA amplification pathway works. RNA slicing by Piwi proteins and that occurring during RNA interference (RNAi) (Meister, 2013) are biochemically indistinguishable. However, RNAi leads to complete degradation of the target. Germ cells must therefore possess an undefined machinery that safely transfers the Piwi-generated slicer cleavage fragments from one ping-pong Piwi partner to the other for maturation as secondary piRNAs. Genetic and biochemical analyses have uncovered a number of factors that are essential for secondary piRNA biogenesis (Czech et al., 2013; Malone et al., 2009), but how they contribute to what is likely to be a multistep processing pathway is currently unclear. RNA helicases are prime candidates for bringing about dynamic associations and remodeling of ribonucleoprotein (RNP) complexes during a variety of RNA processing reactions (Linder and Jankowsky, 2011), and they are among the list of known piRNA biogenesis factors (Figure S1A available online). Among these, we focused our attention on the DEAD box RNA helicase Vasa, as it is the only factor with a conserved role in secondary biogenesis in both flies and mice (Kuramochi-Miyagawa et al., 2010; Malone et al., 2009). *vasa* was originally identified as a maternal-effect gene that is required for development of the female germline in *Drosophila* (Lasko and Ashburner, 1988; Schupbach and Wieschaus, 1986). Like other members of the DEAD box family, Vasa is demonstrated to have ATPase, RNA binding, and RNA unwinding activities (Liang et al., 1994; Sengoku et al., 2006), but its molecular role in the piRNA pathway is not known.

Here, we explored the in vivo function of Vasa using the insect ovarian cell culture model *Bombyx mori* BmN4 (Kawaoka et al., 2009). RNA helicases like Vasa are ATP-gated RNA-binding proteins that engage in dynamic associations. We used a point mutation (DQAD) within the DEAD box of Vasa to prevent release of ATP hydrolysis products, locking the protein onto its bound RNA targets and reducing its in vivo dynamics. Surprisingly, this also trapped a piRNA amplification complex that provides detailed insight into how endonucleolytic cleavage during transposon silencing is linked to generation of a new secondary piRNA. This transiently assembled complex, which we named Amplifier, includes Vasa, the two ping-pong Piwi partners, and the tudor protein Qin/Kumo. Biochemical and structural data reveal that RNA clamping on transposon transcripts by Vasa creates a binding platform for Amplifier components at the surface of Vasa's helicase domain, which is in its ATP-bound, closed conformation. ATP hydrolysis by Vasa opens the helicase domains, resulting in Amplifier disassembly and safe handover of sliced 5′ processed precursors between Piwi proteins for further maturation into piRNAs. Genetic experiments in flies underscore the importance of this ATP-controlled process for fertility. Our results provide detailed mechanistic insight into how transposon cleavage fragments are utilized for generating new piRNAs that preserve genome integrity in the germline.

RESULTS

Comprehensive Transcriptome of the BmN4 Cell Line

The *Bombyx mori* (silkworm) ovary-derived BmN4 cell line is the only cell culture model for piRNA research that has an active ping-pong cycle in operation. These cells express two Piwi proteins—Siwi (Aub ortholog in *Bombyx*) and Ago3—that associate with piRNAs bearing sequence signatures consistent with secondary piRNA biogenesis (Kawaoka et al., 2009). To facilitate studies with this cell line, we cataloged the entire set of piRNA pathway factors in BmN4 using de novo assembly of transcriptome sequencing data (Figure S1A). When compared to *Drosophila*, several of the factors essential for both primary and secondary biogenesis (including Vasa) are conserved. However, notable absences include that of the effector protein Squash and nuclear factors like Rhino, Cutoff, and Deadlock, which are needed for piRNA biogenesis from dual-strand (ping-pong) clusters (Chen et al., 2007; Czech et al., 2013; Klattenhoff et al., 2009; Pane et al., 2007) (Figure S1A). The absence of the latter is likely due to the euchromatic nature of piRNA clusters in BmN4 (Kawaoka et al., 2013), precluding the need for these factors, as they serve to access *Drosophila* piRNA clusters that are embedded in constitutive heterochromatin (Brennecke et al., 2007; Klattenhoff et al., 2009). We also did not find any evidence for the existence of a nuclear Piwi pathway in these cells. Overall, these findings reveal that a unique selection of biogenesis factors fuels the ping-pong cycle in BmN4 cells.

A DEAD Box Mutation Reduces In Vivo Dynamics of Vasa

Our initial attempt at understanding *Bombyx mori* Vasa's role in the piRNA pathway consisted of characterizing isolated complexes from transfected BmN4 cells. However, these failed to reveal any interaction with core piRNA pathway components (see below). DEAD box RNA helicases like Vasa are known to mediate dynamic associations as part of multiprotein assemblies in vivo (Linder and Jankowsky, 2011), which might be hard to detect in biochemical experiments due to their transient nature. This prompted us to examine the dynamics of the proteins involved in the ping-pong cycle by live-cell imaging experiments rather than by looking at a steady-state situation.

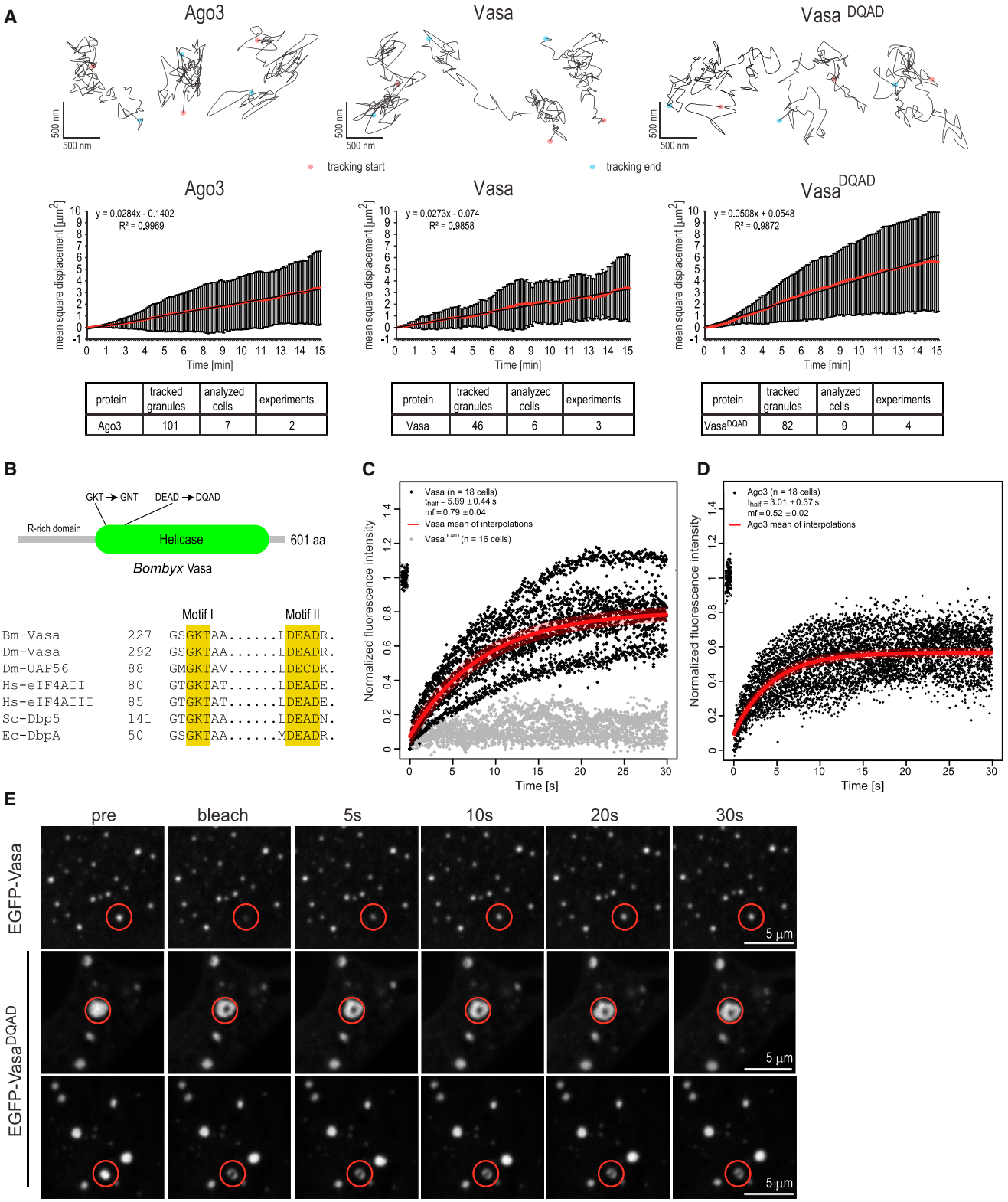

Figure 1. DQAD Mutation in the DEAD Box of Vasa Reduces Its In Vivo Dynamics

(A) BmN4 cells expressing fluorescently tagged Vasa, Vasa^{DQAD}, or Ago3 display abundant cytoplasmic granules, and these were tracked by live-cell imaging. Start and end of tracking is highlighted with a red and blue dot, respectively. Analysis indicates a random, nonlinear movement of these granules, which is unaffected by the DQAD mutation in Vasa.

(legend continued on next page)

Transiently expressed EGFP-Vasa and mCherry-Ago3 colocalize in numerous perinuclear cytoplasmic granules in BmN4 cells. These are analogous to the electron-dense granules called nuage observed in *Drosophila* ovarian nurse cells, which are credited to be piRNA processing centers (Liang et al., 1994; Lim and Kai, 2007). Cell tracking experiments now reveal that, far from being static structures, these display random, nonlinear movements (Figure 1A and Movie S1). More frequently, granules meet to fuse briefly before dissociating, whereas occasionally smaller granules fuse into larger structures. To evaluate the dynamics of the proteins within the nuage, we carried out fluorescence recovery after photobleaching (FRAP) experiments (Movie S2). The measured halftime of fluorescence recovery rates for EGFP-Vasa (5.89 ± 0.44 s) (Figures 1C and 1E) and EGFP-Ago3 (3.01 ± 0.37 s) (Figures 1D, S1B, and S1C) suggest a rapid transit of the proteins through the granules. Thus, any interactions mediated by them within the nuage should be short lived.

Because most activities of RNA helicases are linked to their consumption of ATP (Linder and Jankowsky, 2011), we examined whether abolishing ATPase activity might interfere with the dynamics of Vasa. The DEAD box family is characterized by the presence of a number of sequence motifs within the helicase module (Caruthers and McKay, 2002), prominent among them being the motif II (Asp-Glu-Ala-Asp; D-E-A-D). A single amino acid mutation within this motif (DEAD → DQAD) (Figure 1B) is shown to abolish ATPase activity in other family members (Pause and Sonenberg, 1992). We created a similar mutation within Vasa and expressed its EGFP-tagged version in BmN4 cells. A first indication of an impact of the mutation was the accumulation of EGFP-Vasa^{DQAD} in granules that are slightly larger than those formed by EGFP-Vasa (Figures 1E, 2F, and 2G). Nevertheless, tracking experiments did not reveal any impact of the mutation on the random mobility of the granules (Figure 1A). Strikingly, FRAP experiments showed that fluorescence in Vasa^{DQAD} granules failed to recover, irrespective of the size of the granule examined (Figures 1C and 1E). This is likely to be a consequence of the protein becoming trapped in the granule, preventing further ingress from the surrounding cytoplasm (Movies S3–S5). Thus, an emerging picture is one of highly dynamic events orchestrated within the nuage, which we managed to dampen as a result of the DQAD mutation within Vasa.

Vasa Is Part of a Transient piRNA Amplifier Complex

The retention of Vasa^{DQAD} in enlarged nuage prompted us to ask whether the point mutant might be accumulating in certain complexes in vivo. To this end, we isolated HA-Vasa or HA-Vasa^{DQAD} complexes and identified components by mass spectrometry. The protein arginine methyltransferase 5 (Prmt5 or Capsuleen in *Drosophila*) is common to both complexes, and this is explained by the presence of 20 arginine residues at the N terminus of *Bombyx* Vasa (Figure 2A). Such arginine residues in *Drosophila* Vasa are shown to be targets of Prmt5 for symmetrical dimethyl arginine (sDMA) modifications (Kirino et al., 2010).

Interestingly, HA- and FLAG-Vasa^{DQAD} complexes contained a number of additional factors not present in wild-type Vasa immunoprecipitations (Figures 2A and S2A). In particular, the two most abundant hits among Vasa^{DQAD} interactors are the endogenous ping-pong Piwi partners Siwi (the *Bombyx* ortholog of Aub) and Ago3, which we confirmed by western blot analysis (Figure 2B). Furthermore, tandem immunopurification of FLAG-Vasa^{DQAD} followed by anti-Siwi immunoprecipitation reveals that all three proteins are part of the same entity (Figure 2C). Because the DQAD mutation in Vasa is predicted to prevent ATP hydrolysis, association with Piwi proteins is likely to be favored when Vasa is in its ATP-bound state. To confirm this, we created a mutation in the motif I (GKT → GNT) of the helicase domain that is predicted to prevent ATP binding (Figure 1B). Supporting the requirement for bound ATP, the Vasa^{GNT} mutant did not reveal any association with endogenous Piwi proteins (Figure 2B). The Tudor domain-containing protein Qin/Kumo, a factor essential for the ping-pong cycle (Anand and Kai, 2012; Zhang et al., 2011), was also identified in the Vasa^{DQAD} purifications (Figure 2A). We confirmed this result by western analysis using rabbit polyclonal antibodies to the endogenous Qin/Kumo expressed in BmN4 cells (Figures 2D and S2B). Because all of the validated components are involved in piRNA amplification, we called this Vasa-Siwi-Ago3-Qin/Kumo complex Amplifier.

Arginine methylation of Piwi proteins is shown to act as an affinity enhancer for mediating protein-protein interactions (Mathioudakis et al., 2012), so we wondered whether Vasa methylation plays any role in Amplifier assembly. Pointing to the absence of such a role, when we mutated all of the N-terminal arginines (to lysines; R → K) in Vasa^{DQAD}, the interaction with the Amplifier components was still maintained, as examined by mass spectrometry and western blot analysis (Figures 2A and 2E). In contrast, recovery of Prmt5 was abolished in both *Bombyx* Vasa$^{R\text{-}K}$ and Vasa$^{DQAD(R\text{-}K)}$ purifications (Figure 2A). We propose that the Amplifier complex is assembled on wild-type Vasa, but its transient nature prevents its detection (Figure S2C). However, the DQAD mutation in Vasa freezes this complex by preventing its disassembly, thereby allowing its identification.

Amplifier Assembly Takes Place within the Nuage

In BmN4 cells, Vasa and Ago3 are nuage residents, while the vast majority of Siwi is present diffused in the cytoplasm (Xiol et al., 2012). To examine where in the cell they might transiently associate, cells expressing HA-tagged Vasa proteins were counterstained for endogenous Amplifier components using specific

(B) Sequence alignment of DEAD box helicases showing critical residues for ATP binding (motif I) and ATP hydrolysis (motif II). Point mutations within *Bombyx* Vasa used in this study are indicated in the cartoon.

(C) Recovery of fluorescence after photo bleaching (FRAP) of EGFP-Vasa or EGFP-Vasa^{DQAD} granules is indicated as a function of time (in seconds, s).

(D) Recovery times for EGFP-Ago3.

(E) Time series snapshots (time in seconds, s) focusing on the granules in the cytoplasm from FRAP experiments conducted with BmN4 cells expressing indicated fluorescently labeled proteins. The bleached granule is indicated with a red circle. Note that Vasa^{DQAD} granules are generally larger but show a range of sizes, with the middle panel showing a granule where the laser photobleaches the center of the granule.

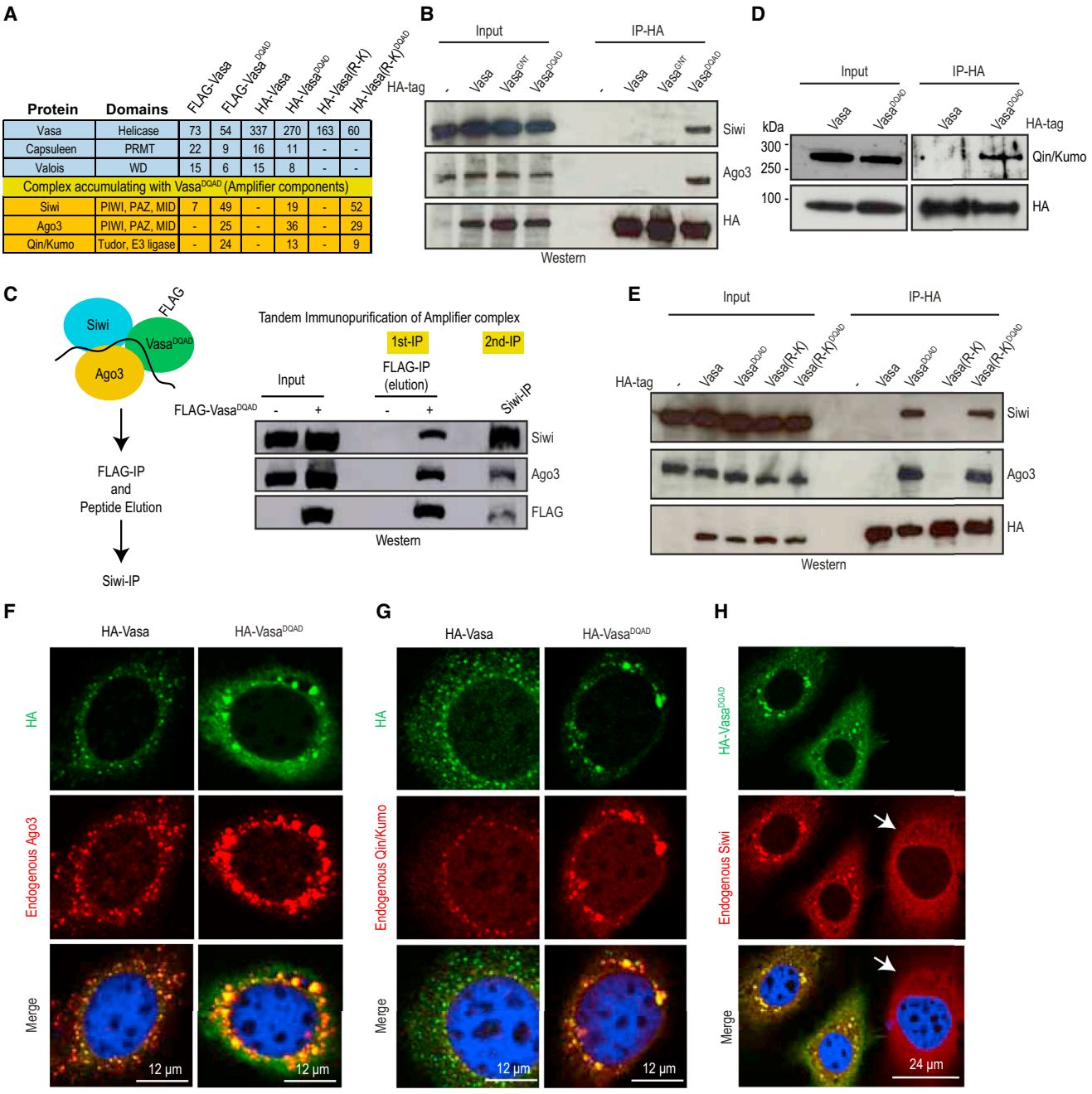

Figure 2. A Transient piRNA Amplifier Complex Containing Vasa Is Assembled in the Nuage

(A) Mass spectrometry analyses of indicated tagged protein complexes isolated from transiently transfected BmN4 cells. Note that Prmt5/Capsuleen is common to both Vasa and Vasa^{DQAD}, though the latter has a unique set of factors (see Figure S2A for a complete list), including ping-pong Piwi proteins and Qin/Kumo, which were validated by western blotting analyses. A ratio of spectral counts in the sample versus beads control is indicated.

(B) Immunoprecipitation and western blot analysis confirming specific association of endogenous Piwi proteins Siwi and Ago3 with HA-Vasa^{DQAD}.

(C) Tandem affinity purification showing presence of Vasa^{DQAD} and the ping-pong Piwi partners in the same complex.

(D) Western blot analysis showing specific association of endogenous Qin/Kumo with HA-Vasa^{DQAD}.

(E) Mutation of 20 N-terminal arginines to lysines (R–K) in Vasa^{DQAD} does not affect Amplifier assembly but abolishes recovery of Capsuleen (see A).

(F–H) Accumulation of Vasa^{DQAD} in large nuage in BmN4 cells that are also enriched in endogenous Amplifier components like Ago3 (F), Qin/Kumo (G), and Siwi (H). Note that, in untransfected cells lacking HA-Vasa^{DQAD} (white arrow in H), Siwi remains dispersed in the cytoplasm. Scale bars (in µm) are indicated.

antibodies. We find that, like endogenous Ago3 (Figure 2F), Qin/Kumo (Figure 2G) also accumulates in cytoplasmic granules that also contained HA-Vasa, whereas Siwi is spread out in the cytoplasm (Figure 2H). Interestingly, examination of the endogenous proteins in cells expressing HA-Vasa^{DQAD} shows that the enlarged nuages formed by Vasa^{DQAD} also contained a higher enrichment of Ago3 and Qin/Kumo (Figures 2F, 2G, and S2D). Furthermore, cytoplasmic Siwi was now concentrated in these perinuclear granules. The redistribution of Siwi from the cytoplasm to the granules is striking, given the almost complete absence of Siwi granules in untransfected or HA-Vasa-expressing cells (Figures 2H, S2E, and S2F). The above experiments suggest that all of the factors enter the nuage from the surrounding cytoplasm to assemble the Amplifier and then exit after execution of their functions (Figure S2G). Nevertheless, we cannot rule out the possibility that complex assembly may already take place in the cytoplasm, but its eventual disassembly (which is blocked by the DQAD mutation in Vasa) definitely takes place within the nuage.

Amplifier Contains Antisense piRNAs and Sense Transposon Targets

Given the presence of Piwi proteins in the Amplifier complex and to get an insight into its function within the nuage, we examined the presence of small RNAs in Vasa^{DQAD} complexes. To this end, we immunoprecipitated HA-tagged Vasa complexes from BmN4 cells and revealed the presence of small RNAs by 5′ end labeling and 20% polyacrylamide gel electrophoresis (PAGE). Small RNAs consistent with the length of piRNAs (~30 nt) are observed in Vasa^{DQAD} purification, but not in Vasa and Vasa^{GNT} complexes (Figure 3A). As previously shown for Piwi proteins (Figures 2A and 2E), small RNA association with Vasa^{DQAD} is also independent of Vasa arginine methylation (Figure S3A). Surprisingly, another smeary RNA species of ~12 nt was also abundantly detected in Vasa^{DQAD} complexes (Figures 3A and 3B).

To uncover the identity of the short RNAs, we subjected them to deep sequencing (Figure 3B). The ~30-mer RNA species (duplicate libraries) have a read-length profile (peak at 27 nt) similar to that reported for *Bombyx* piRNAs (Figure S3B). They also display the characteristic nucleotide biases seen in piRNAs, such as preference for a uridine at the 5′ end (1U-bias, ~85%) and presence of an adenosine at position 10 (A10-bias, ~40%) (Figure S3C). Based on comparison to available Siwi and Ago3 piRNA libraries (Xiol et al., 2012), ~75% of the reads in the Amplifier complex can be classified as piRNAs (hereafter referred to as Amplifier-piRNAs) (Figure 3C). Next, we wished to ascertain whether these piRNAs represent those bound to Siwi or Ago3, as this could help in determining the position of Amplifier within the ping-pong cycle. This task is complicated by the fact that the bulk of the reads is shared between Siwi and Ago3 libraries when only sequence identity is considered. However, when their relative abundance (see Extended Experimental Procedures) in a particular library is also accounted for, the reads can be sorted as belonging to either Siwi or Ago3. Based on this calculation, piRNAs from Siwi accounted for the majority in the Amplifier-piRNA pool (~75%) (Figure 3C). This is also evident when the reads are aligned on transposon consensus sequences. Amplifier-piRNA reads have a predominant antisense bias very much like Siwi piRNAs, whereas those in Ago3 map to the sense strand (Figure 3D-E). Thus, Amplifier contains essentially Siwi-bound antisense piRNAs (Figure 3F).

Next, we prepared two independent deep-sequencing libraries for the abundantly present 12-mer species (median size of 12 nt) (Figure 3B). Mapping short reads like 12-mers can give multiple genomic hits, preventing unambiguous annotation. Therefore, we confined our search to transposon consensus sequences, allowing only perfect matches. Strikingly, the 12-mer reads predominantly mapped to the sense strand of the transposons (Figure 3E). This opposing polarity with Amplifier-piRNAs (that map to the antisense strand) is maintained over several *Bombyx* transposon sequences (Figure 3F). The short size of the 12-mers and their smeary nature suggests that these might be in vivo RNA footprints left by Vasa on bound transposon transcripts after degradation by cellular nucleases. In agreement with this, a recombinant preparation of Vasa^{DQAD} containing only the helicase core domain generates footprints (~6–10 nt) on a radioactively labeled RNA in vitro (Figure 3G). We conclude that the 12-mers are unlikely to be intermediates of the piRNA biogenesis process but might rather reflect the entire repertoire of RNA-binding sites of Vasa (Figures S3D–S3F and see discussion in Extended Experimental Procedures). To examine the presence of piRNA precursors within Vasa-bound transcripts, we extracted longer RNAs present in Amplifier complexes and prepared a strand-specific RNAseq library (fragment size of ~200 nt). Comparison to the total polyA+ transcriptome from BmN4 cells reveals an enrichment of transposon sequences (Figure 3H). Mapping to transposon consensus reveals these to be predominantly sense-oriented sequences (Figure 3I).

The ping-pong model predicts that the Piwi protein with antisense piRNAs (Siwi in BmN4 cells) facilitates biogenesis of sense-oriented Ago3-bound piRNAs from transposon transcripts (Brennecke et al., 2007). We found that Vasa gathers both Siwi and Ago3 in the nuage to assemble Amplifier, which contains mainly Siwi-bound antisense piRNAs and their target sense transposon transcripts. Considered together, the above results strongly suggest that Amplifier is the biochemical platform for generation of Ago3-bound secondary piRNAs from sense transposon precursors. Consistent with a role for RNA in complex formation, retention of both Siwi and Ago3 in the complex is sensitive to RNase treatment. However, Siwi was the most affected (Figures 3J and S3G), hinting to a requirement for piRNA-mediated base-pairing to the target for its inclusion in the complex.

Amplifier Complex Contains 5′ Processed piRNA Intermediates

There could be two potential roles for Vasa within the Amplifier complex. Vasa might regulate slicer activity of Siwi so that it occurs only after the two ping-pong partners are brought together. This should ensure safe transfer of the sliced precursor fragment, i.e, the secondary piRNA intermediate, from Siwi to Ago3. Alternatively, slicing by Siwi may have already taken place, but transfer of the intermediate to Ago3 requires Vasa to complete ATP hydrolysis.

Because the repeat-rich nature of endogenous piRNAs prevents unambiguous determination of intermediates, we created an artificial secondary piRNA precursor. We identified 14 highly

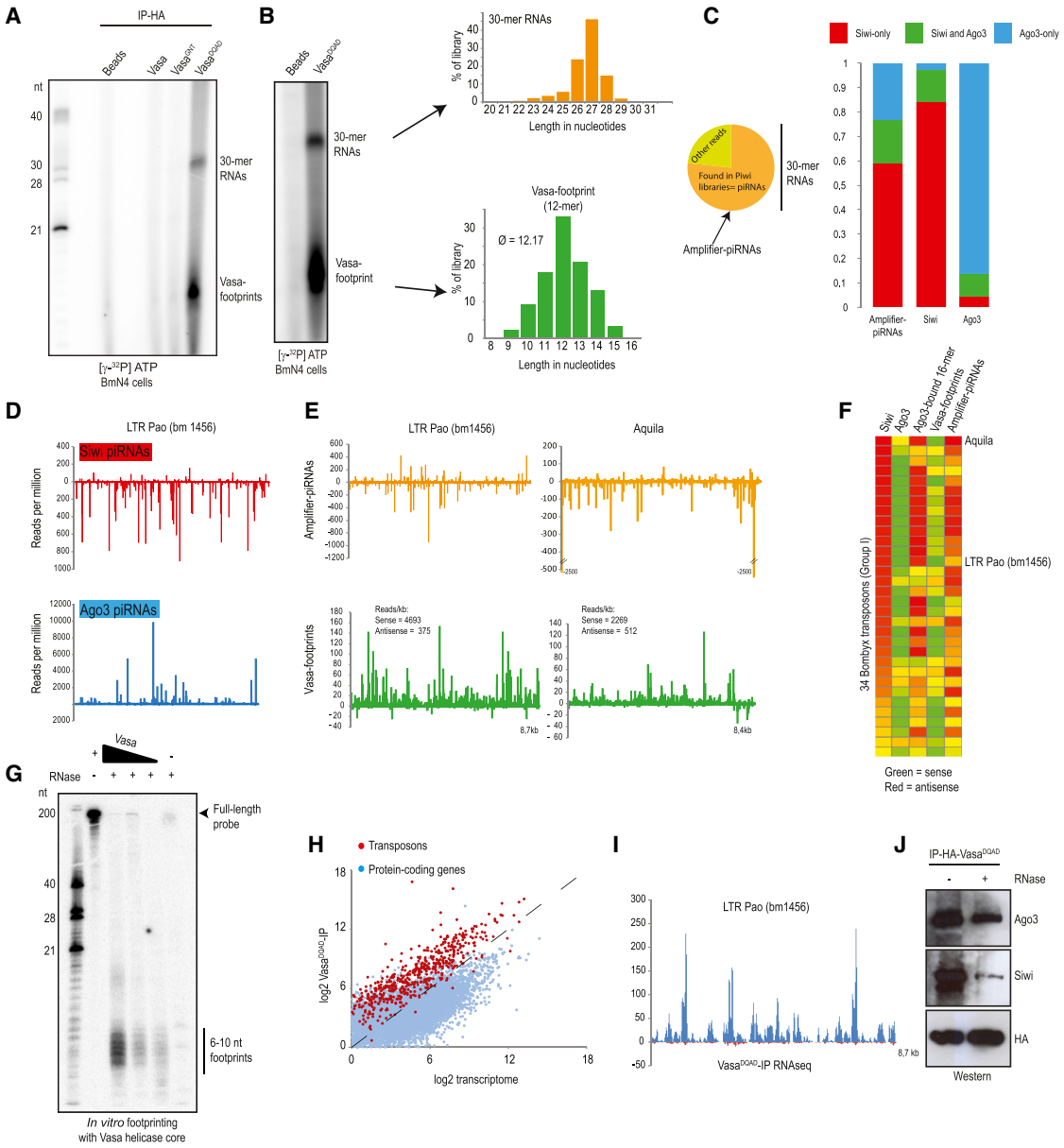

Figure 3. Amplifier Contains Siwi-Bound Antisense piRNAs and Sense Transposon Transcripts

(A) Association of Vasa^{DQAD} with short RNAs in BmN4 cells. The two prominent small RNA species—~30-mer RNAs and ~12-mer Vasa footprints—are identified.

(B) Read-length distribution of indicated RNAs.

(C) Overlap of ~30-mer RNAs with known piRNA libraries identifies ~75% of the reads as piRNAs (Amplifier-piRNAs). Sorting of piRNAs as those associating with the two Piwi proteins using sequence identity and enrichment filters (see Extended Experimental Procedures). The majority of the Amplifier-piRNAs are those associated with Siwi.

(D) Mapping of reads from indicated Piwi libraries on a transposon consensus sequence. Note the opposing polarity of Siwi- and Ago3-associated reads.

(E) Mapping of reads on two transposon consensus sequences. Note the opposing polarity of Amplifier-piRNAs and Vasa footprints.

(F) Heatmap showing strand bias of reads from Siwi, Ago3, Vasa-footprints, and Amplifier-piRNAs on 34 *Bombyx* transposon consensus sequences. Ago3-bound 16-mer refers to byproducts originating from Siwi piRNA precursors and has same strand orientation as Siwi piRNAs (Xiol et al., 2012).

(G) In vitro footprint generated by recombinant core helicase domain of Vasa^{DQAD} on a radioactively labeled RNA probe.

(H) Enrichment of transposon sequences within Amplifier (Vasa^{DQAD}-IP) complexes when compared to the general PolyA+ transcriptome of BmN4 cells.

(I) The Amplifier-bound (Vasa^{DQAD}-IP) transposon reads are mainly mapping to the sense strand of the indicated transposon consensus sequence.

(J) Presence of Piwi proteins in Amplifier (Vasa^{DQAD}) complexes is sensitive to RNase treatment. Note that Siwi is more sensitive to the treatment than Ago3. See also Figure S3G.

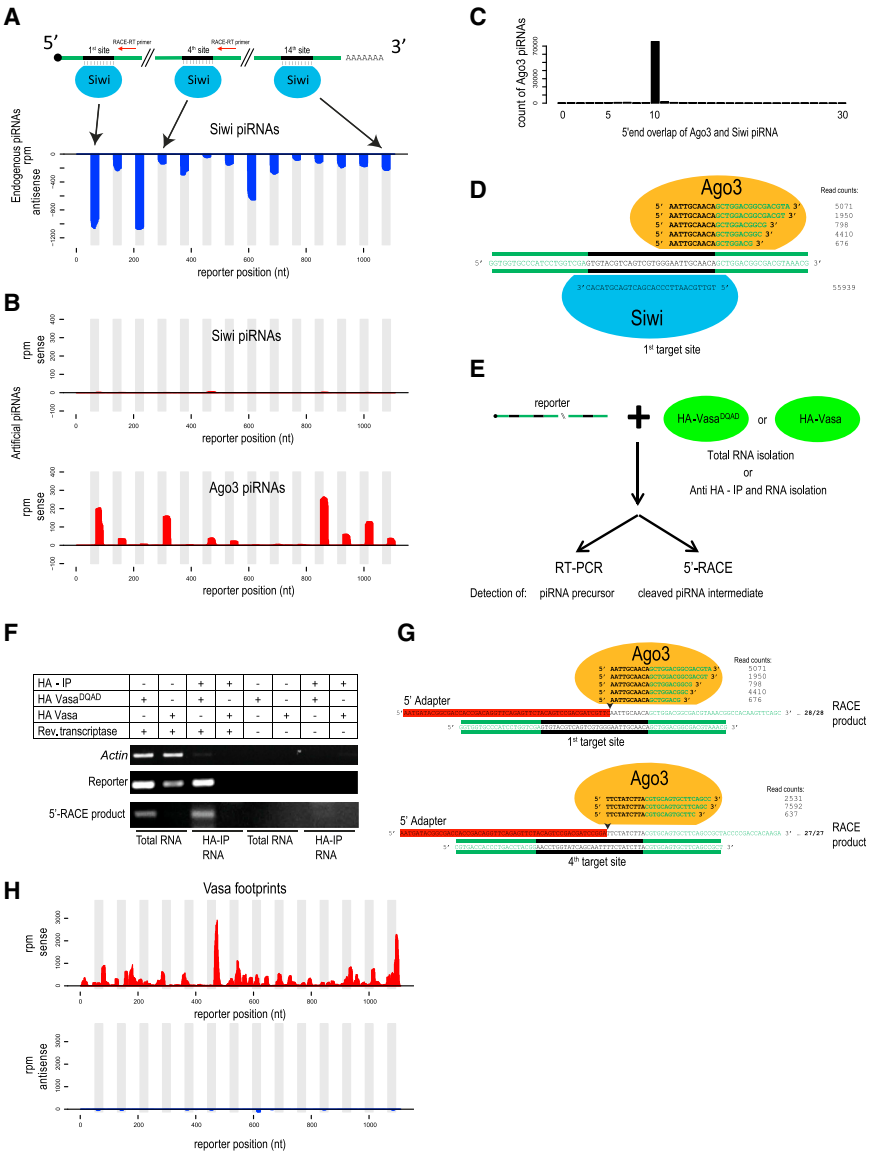

Figure 4. Amplifier Contains 5′ Processed Secondary piRNA Intermediates

(A) Design of the artificial secondary piRNA precursor. The noncoding green fluorescent protein (GFP) sequence has perfectly complementary binding sites for 14 piRNAs abundantly present in endogenous Siwi complexes in BmN4 cells. Details of three such targeting sites and placement of reverse-transcription primers used for RACE experiments (RACE-RT primer) are shown. Shown below is a density plot (reads per million, rpm) of Siwi-bound piRNAs complementary to the artificial precursor. The shaded regions indicate the Siwi-piRNA-binding sites on the reporter.

(B) Endogenous Piwi proteins (Siwi and Ago3) were isolated from BmN4 cells expressing the reporter and presence of reporter-derived sequences (sense; shown in red) examined. Reporter-derived piRNAs are specifically sorted into endogenous Ago3 complexes, but not Siwi.

(C) The reporter-derived Ago3-bound piRNAs have their 5′ ends overlapping exactly by 10 nt with that of Siwi-bound antisense piRNAs, indicating their origin from Siwi slicing of the reporter.

(D) Reporter-dervied piRNAs are truly artificial, as they are chimeric with 10 nt of *Bombyx* repeat sequence (in black) and ~16 nt of GFP sequence (in green).

(E) Experimental setup to assay for presence of reporter RNA (by RT-PCR) or of piRNA intermediate (by 5′-RACE) in Vasa complexes or total cellular RNAs.

(F) Detection of reporter RNA or piRNA intermediate (5′-RACE product). Control reactions carried out without added reverse transcriptase is also shown.

(G) Sanger sequencing of 5′ RACE products, revealing their 5′ ends (marked with an arrowhead) to be exactly the same as those of mature reporter-derived Ago3-bound piRNAs (for example, in 28 of 28 sequenced clones for first target site). The sequence highlighted in red is the 5′ adaptor used for cloning RACE products. The relevant portion of the reporter sequence is shown below.

(H) Mapping of Vasa footprints on reporter.

abundant Siwi piRNAs and placed perfectly complementary binding sites for these (spaced by ~50 nt) in the context of a noncoding (all ATGs removed) green fluorescent protein (GFP) sequence (Figure 4A) and expressed it in BmN4 cells. We then monitored the presence of reporter-derived piRNAs in endogenous Siwi and Ago3 complexes by deep sequencing (two independent libraries for each protein) (Figure S4A).

Mapping of reads (perfect match only) to the reporter sequence indicates the expected presence of antisense piRNAs in Siwi, and these are complementary to the inserted binding sequences (Figure 4A). Such antisense reads are also found in Ago3 libraries (Figure S4B) but with fewer read counts, again highlighting the difficulty of accurately assigning endogenous repeat piRNAs to distinct ping-pong partners. Significantly, reporter-derived (sense) piRNA sequences are found exclusively in the Ago3 libraries (Figure 4B). Such reads are nonrandomly distributed on the sense strand and map at specific sites across from the complementary Siwi piRNAs. Confirming their origin from Siwi-guided slicing of the reporter, the 5′ ends of sense reporter reads in Ago3 display an overlap of 10 nt with that of the complementary Siwi piRNAs (Figure 4C). The sense reads thus generated are truly artificial secondary piRNAs, as it is a chimera between *Bombyx* repeat sequence (1–10 nt) and the GFP backbone (11–26 nt) (Figure 4D). Thus, the reporter is a genuine precursor for Siwi-guided biogenesis of secondary piRNAs associating with Ago3. To examine the presence of the reporter within the Amplifier complex, we coexpressed the reporter and HA-tagged Vasa proteins in BmN4 cells. After anti-HA purifications, we examined the presence of the reporter sequence by RT-PCR analysis (Figure 4E). The reporter was easily detected in HA-Vasa^{DQAD} complexes, but not in HA-Vasa purifications, again reflecting the dynamic nature of the process (Figure 4F).

Next, we examined the presence of secondary piRNA processing intermediates within the Amplifier complex. Slicer cleavage by Argonautes like Siwi is expected to generate two fragments: one with a 5′ monophosphate and another carrying a 3′ hydroxyl (OH) group at the site of cleavage (Meister, 2013). The former (piRNA intermediate) is utilized to generate a secondary piRNA, whereas the latter is discarded. Taking advantage of the presence of a 5′ phosphate on the piRNA intermediate fragment, we attempted 5′ RACE experiments to detect these (Figures 4A and S4C). This revealed the specific presence of RACE products only in RNA isolated from the Vasa^{DQAD} complex (Figure 4F). Significantly, Sanger sequencing revealed that 100% of the 5′ RACE products (28 out of 28 sequenced clones for first target site) contain 5′ ends that are generated by Siwi slicer cleavage and match precisely to that of mature Ago3-bound reporter-derived piRNAs (Figure 4G). This strongly suggests that Amplifier contains piRNA intermediates with an already defined 5′ end that are awaiting further 3′ processing after loading into Ago3. Identical results were obtained in RACE experiments that were carried out for detection of another intermediate (at target site 4) (Figure 4G) in independent transfection experiments. Interestingly, 5′ processed piRNA intermediates (RACE products) are also detected in total RNA from cells expressing HA-Vasa^{DQAD}, but not from those expressing HA-Vasa (Figure 4F), even though they are a necessary intermediate for producing mature secondary piRNAs found in Ago3 (Figure 4B). This is likely explained by the fact that, in the latter situation, piRNA intermediates are transferred to Ago3 and are rapidly processed, whereas in the case of cells expressing HA-Vasa^{DQAD}, these are trapped in the Amplifier complex, allowing its efficient detection even in total cellular RNAs. Finally, mapping of the Vasa footprints on the reporter sequence reveals peaks that cluster around the ping-pong sites (Figures 4H and S4D). This indicates that Vasa physically binds to the secondary piRNA intermediate for safely transferring it to Ago3 for maturation. Thus, although target slicing by Siwi has already taken place in the snapshot of Amplifier that we have frozen, handover of the cleavage fragment to Ago3 and maturation of the fragment as a new secondary piRNA fail to occur in the absence of ATP hydrolysis/disassembly of the complex by Vasa.

The DQAD Mutation in Vasa Prevents Release of ATP Hydrolysis Products

Our cell culture experiments point to an important role for Vasa's ATPase cycle in regulating Amplifier assembly, as we were able to trap this complex only by using a mutation that is predicted to abolish its ATPase activity. We therefore took an in vitro approach to gain molecular insight into this process. We prepared recombinant versions of *Bombyx* Vasa containing only the helicase core domain (135–564 aa) (Figure S5A). As expected from studies of other DEAD box helicases (Pause and Sonenberg, 1992), the Vasa^{GNT} mutant failed to bind ATP, whereas both Vasa and Vasa^{DQAD} showed binding in an UV crosslinking assay (Figure 5A). We note that Vasa^{DQAD} consistently gave stronger signals in the ATP-binding assays. Vasa and Vasa^{DQAD} also displayed ATP-stimulated binding activity to a poly-U RNA (Figure S5B). The DQAD mutation in eIF4A, a prototypic member of the DEAD box helicase family, is reported to abolish its ATPase activity (Pause and Sonenberg, 1992), so we were surprised to find that Vasa^{DQAD} still retained catalytic activity, as assayed in our low-substrate conditions (Figure 5B). We conclude that Vasa^{DQAD} behaves very much like the wild-type protein in the in vitro experiments, leaving us with no explanation for the observed in vivo effects. This prompted us to take a closer look at the helicase core by X-ray crystallography (Figure S5C and Extended Experimental Procedures).

We were able to determine the structure of *Bombyx* Vasa^{DQAD} helicase core domain in complex with a 6 nt RNA and ATP at 2.1 Å resolution. The structure of the wild-type version of the *Drosophila* ortholog had been previously determined in the presence of a nonhydrolyzable ATP analog AMPPNP (Sengoku et al., 2006), likely reflecting the need to freeze the protein in an ATP-bound state in order to perform crystallographic studies. The BmVasa^{DQAD}-RNA-ATP structure revealed the two RecA-like domains in a closed conformation, with the ATP-binding site created in the cleft between them. The characteristically bent RNA contacts both the RecA-like domains and is held in a position opposite to the ATP-binding pocket (Figure 5C). The overall architecture is similar to that found in wild-type *Drosophila* Vasa (Figure S5D) (Sengoku et al., 2006), and our second *Bombyx* Vasa^{DQAD} structure with AMPPNP shows that the catalytic water is correctly positioned prior to ATP hydrolysis (Figures S5E and S5F).

Surprisingly, in the structure obtained from crystals containing added ATP, the ligand was hydrolyzed and the products (ADP and γ-phosphate [Pi]) were retained in the protein (Figures 5C and S5G). ATP hydrolysis products are normally released from ATPases and are not observable within RNA helicases, as they promote recycling of the enzyme (Liu et al., 2008). Our structure now provides the basis for retention of the hydrolysis products within Vasa^{DQAD}. First, the mutation (E339Q) converts the negatively charged side chain of glutamate (E) to a neutral charge in glutamine (Q), removing a repulsive force that would normally be used to eject the negatively charged γ-phosphate. Second, the free phosphate is held in place by hydrogen bonding with a number of residues, with the mutated residue Q339 in Vasa^{DQAD} providing an additional interaction that is not available in the native context (Sengoku et al., 2006) (Figure 5C). Failure to release hydrolysis products can prevent turnover of the enzyme (Liu et al., 2008), perhaps explaining the increased crosslinking of ATP to the protein (Figure 5A) and reduced ATPase activity under high substrate concentrations (Figure S5H). Thus, we conclude that Vasa^{DQAD} is a product-release-trap mutant.

ATP-Gated RNA Clamping by Vasa Allows Amplifier Assembly on Its Helicase Core Domain

Next, we asked how failure to release ATP hydrolysis products by Vasa contributes to the observed in vivo effects in BmN4 cells. DEAD box helicases are ATP-gated RNA-binding proteins; ATP binding promotes the closed conformation of the two RecA-like domains, and this translates into a tight binding to the RNA, whereas ATP hydrolysis releases this grip (Linder and Jankowsky, 2011). The fact that RNA intermediates of the ping-pong cycle are detected in Amplifier (Figure 4F) prompted us to look at the dynamics of RNA binding by Vasa. We used surface plasmon resonance (SPR) experiments to monitor the dynamics of Vasa affinity for single-stranded RNA in the presence of ATP

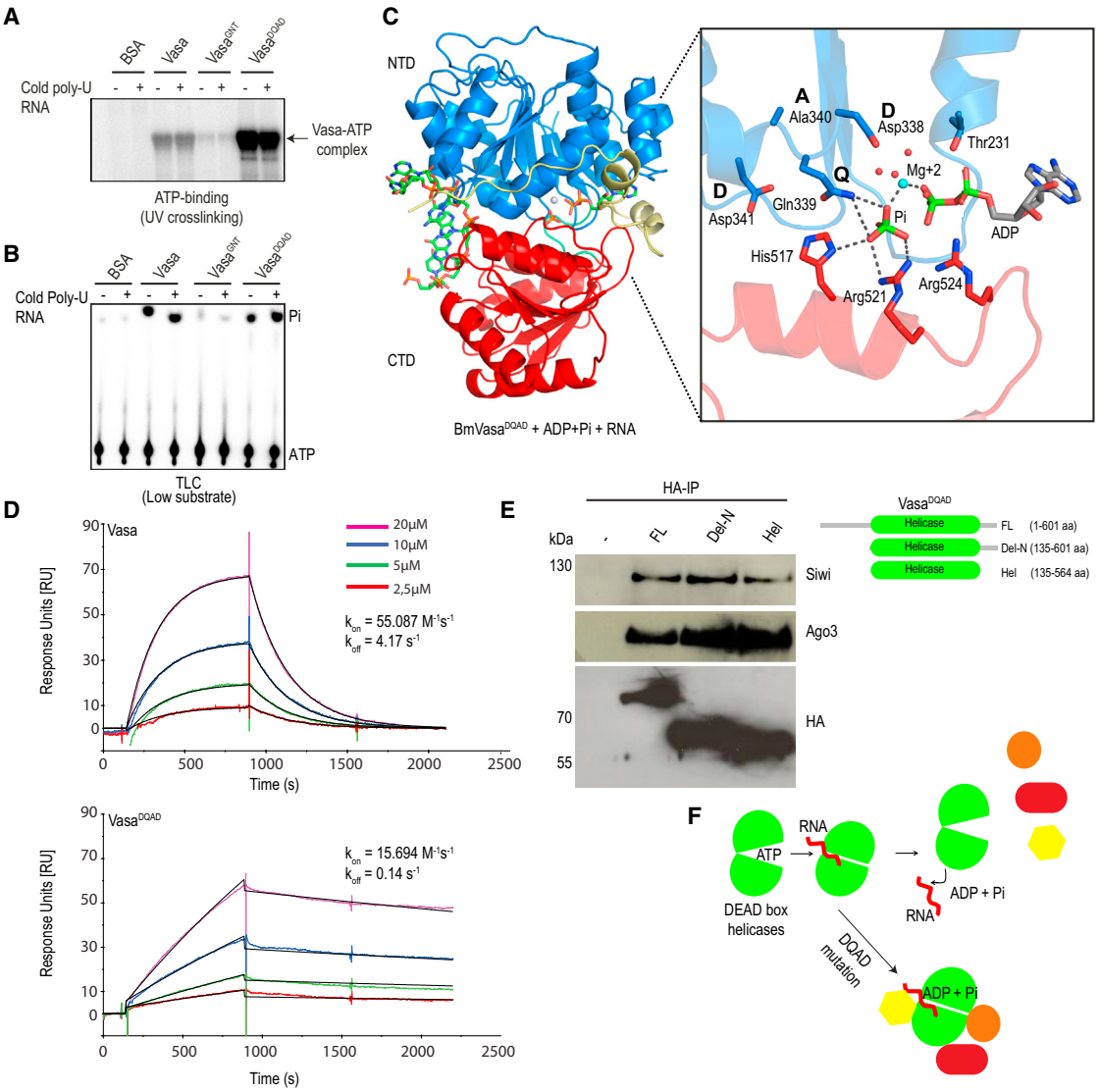

Figure 5. The ATP-Bound Closed Conformation of Vasa's Core Helicase Domain Provides a Platform for Amplifier Assembly

(A) UV crosslinking assay to detect ATP binding with recombinant *Bombyx* Vasa helicase domains carrying the indicated mutations. Bovine serum albumin (BSA) serves as a negative control. Reactions were carried out in the presence (+) or absence (–) of unlabeled (cold) poly-U RNA.

(B) ATP hydrolysis assays to reveal generation of inorganic phosphate (Pi). Low substrate; indicates that reactions contained only radioactive ^{32}P-γ-ATP, without added cold ATP. See also Figure S5H.

(C) Crystal structure of *Bombyx mori* (Bm) Vasa^{DQAD}-RNA-ADP-P$_i$ complex. The two recA-like domains (blue and red) of the helicase module are represented as ribbons, whereas RNA and ATP are indicated as ball-and-sticks. ATP added during crystallization with BmVasa^{DQAD} becomes hydrolyzed into ADP and Pi. Interaction with glutamine (Q339) traps Pi in the protein, creating a product-release mutant. Magnesium ion (Mg^{2+}) (blue ball) and water molecules (red balls) are indicated.

(D) Surface plasmon resonance (SPR) experiments indicate that both proteins have similar RNA-binding kinetics (k_{on}), but Vasa^{DQAD} shows drastically slower off rates (k_{off}). Interactions were examined at different protein concentrations (different line colors), and binding to RNA is reported in arbitrary response units (RU) as a function of time (in seconds, s).

(E) Deletion constructs of HA-Vasa^{DQAD} were transfected into BmN4 cells and association of endogenous Piwi proteins examined by western blotting.

(F) A model showing consequence of DQAD mutation for DEAD box proteins. The mutation traps helicases in the closed conformation, freezing bound RNA and protein complexes.

(Figure 5D). Both Vasa and Vasa^{DQAD} bound RNA with rather similar kinetics (K_{on}). However, the off rate for Vasa^{DQAD} (K_{off} = 0.14 s^{-1}) was ~40-fold lower than that of Vasa wild-type (K_{off} = 4.17 s^{-1}), indicating very tight binding to RNA. This indicates that the inability to release ATP hydrolysis products and the consequential enforcement of the closed conformation of Vasa^{DQAD} traps it on bound RNAs, which we identified as sense piRNA precursors (Figure 3H). Interestingly, our biochemical

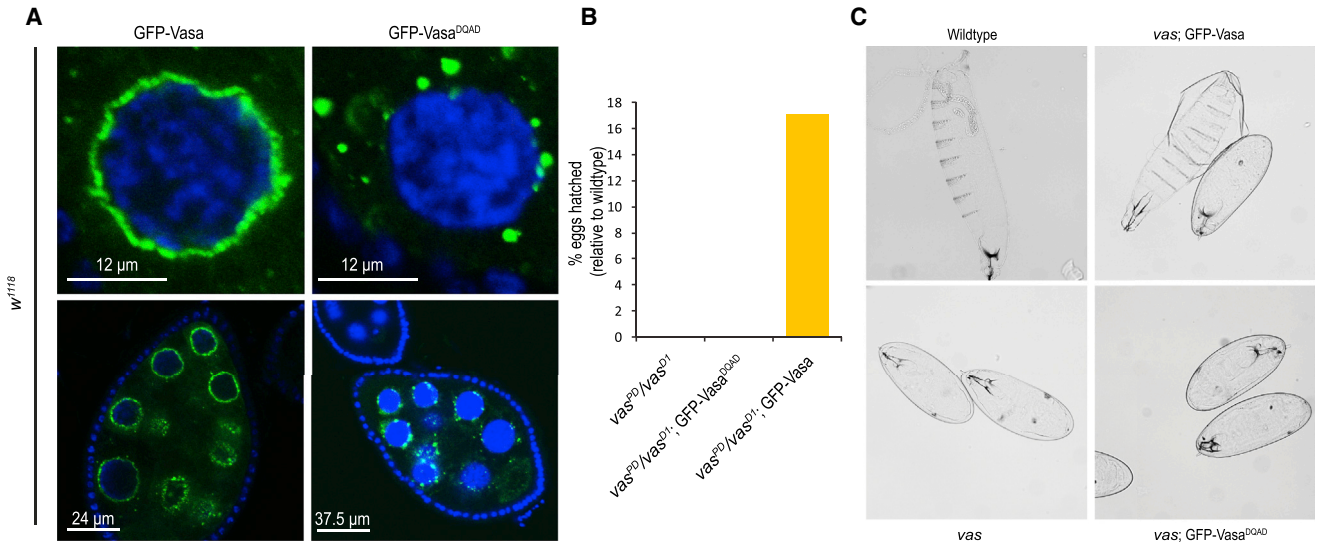

Figure 6. ATP Hydrolysis by Vasa Is Essential for Fertility in *Drosophila* Females

(A) Fluorescence detection of GFP fusion proteins in transgenic fly ovaries in the wild-type genetic background. GFP-DmVasa^{DQAD} accumulates in granules that are removed from the regular perinuclear ring-like nuage localization, potentially indicating an impact on the in vivo dynamics of the protein.

(B) Eggs laid by the *vas* mutant fail to hatch, and this is rescued by a GFP-Vas transgene, but not by the GFP-DmVasa^{DQAD} transgene. Number of eggs hatched is indicated as a percentage of that seen in the wild-type. The partial rescue (~16%) is explained by the fact that the transgenes are expressed from a nonnative promoter.

(C) Cuticle staining of such hatched embryos shows the segmentation pattern expected of normal development (in wild-type and *vas* mutants complemented with GFP-Vas).

experiments (Figures 2A–2E) in BmN4 cells suggest that such an ATP-bound and RNA-clamped state of Vasa also provides a binding platform for Amplifier assembly.

Vasa has a rather simple architecture with an N-terminal arginine-rich region (R-rich domain), followed by the canonical DEAD box helicase core domain (Figure 1B). To understand how Vasa can mediate Amplifier assembly, we prepared deletion constructs and examined their ability to support association with other factors in vivo. Transiently expressed deletion constructs were purified by anti-HA immunoprecipitations and probed with antibodies to detect endogenous Piwi proteins. Deletion of the R-rich domain (1–134 aa) did not affect association with Siwi and Ago3 (Figure 5E). This adds to our observation that N-terminal arginines in Vasa are not required for mediating complex formation (Figures 2A and 2E). Remarkably, a construct having only the helicase core domain was capable of associating with Siwi and Ago3 (Figure 5E), indicating that Amplifier is assembled on the surface of the helicase core of Vasa. We propose that the binding interface for Amplifier components is created only when the helicase domain is in a closed conformation and, consequently, only when Vasa is bound to its target RNAs (Figure 5F). Subsequent ATP hydrolysis would promote release of the RNA and would result in an open conformation of the helicase domain, disrupting the protein interaction surface and leading to complex disassembly.

ATP Hydrolysis by Vasa Is Essential for Fertility in the *Drosophila* Female Germline

Impaired piRNA pathway leads to infertility in all animal models, including in *Drosophila vasa* (*vas*) mutants (Malone et al., 2009). Because the DQAD mutation within *Bombyx* Vasa prevents Amplifier disassembly, we wished to examine whether such a mutation within *Drosophila* Vasa might have a functional consequence for fly fertility. We expressed *Drosophila* Vasa transgenes (GFP-Vas or GFP-Vas^{DQAD}) in wild-type *Drosophila* ovaries (Figure S6A). Whereas GFP-Vas localized as a perinuclear ring to the nuage of nurse cells (Lasko and Ashburner, 1988), GFP-Vas^{DQAD} protein appeared to form distinct foci that are removed from the perinuclear location (Figure 6A). These are reminiscent of enlarged granules observed in BmN4 cells (Figures 1E, 2F, and 2G). Next, we expressed the transgenes in the *vas^{PD}/vas^{D1}* mutant background (these mutants lay eggs that fail to hatch) (Lasko and Ashburner, 1988). When GFP-Vas is expressed in the mutant background, it complements infertility (Figures 6B, S6A, and S6B). The rescued embryos showed normal segmentation patterns, very similar to those hatched from eggs laid by wild-type females (Figure 6C). Significantly, the GFP-Vasa^{DQAD} transgene failed to rescue the infertility phenotype of the mutant (Figures 6B and 6C and Extended Experimental Procedures). These experiments provide strong genetic evidence for the physiological effect of preventing disassembly of Vasa RNPs in the *Drosophila* germline.

DISCUSSION

Secondary piRNA biogenesis (the ping-pong cycle) links post-transcriptional silencing of transposons by Piwi endonucleases to piRNA biogenesis by converting one of the cleavage fragments into a new secondary piRNA (Brennecke et al., 2007; Gunawardane et al., 2007). This poses a unique problem, as

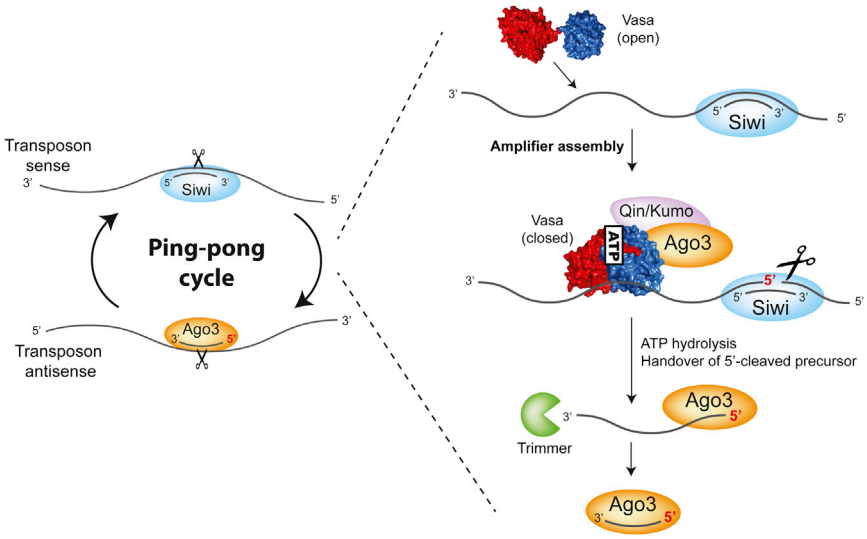

Figure 7. A Model for Vasa's Role in the Ping-Pong Cycle

Recognition of transposon transcripts by Siwi-bound antisense piRNAs is proposed to result in recruitment of Vasa. The open conformation of Vasa's helicase domain is modeled on the eIF4A structure (PDB: 1FUU). Vasa binds RNA in its ATP-bound form, taking up a closed conformation of its RNA helicase domain. This closed conformation also provides an assembly platform for Amplifier components (ping-pong Piwi partners and the Tudor domain protein Qin/Kumo). After Siwi slicing of the transposon transcript, the cleavage fragment carrying the 5′ monophosphate (piRNA intermediate) is transferred to Ago3. ATP hydrolysis in Vasa triggers this exchange and eventual disassembly of the Amplifier. Subsequently, the piRNA intermediate is subject to 3′ end maturation by a putative exonuclease (Trimmer) to mature as a new secondary piRNA. Loaded Ago3 then enters the feedforward step of the ping-pong cycle to generate more of the Siwi-bound piRNAs.

endonucleolytic cleavage of a target RNA by an Argonaute normally results in complete degradation of the two resulting cleavage fragments in all cell types. Germ cells must therefore possess an unknown machinery that safely delivers a cleavage fragment (piRNA intermediate) from one Piwi protein to another (ping-pong partners), but the molecular basis for this process is not known. Among the list of over 30 factors that are genetically linked to the piRNA pathway (Figure S1A), we chose to investigate Vasa, as it is the only factor that is demonstrated to have a conserved and exclusive role in secondary piRNA biogenesis in flies and mice (Kuramochi-Miyagawa et al., 2010; Malone et al., 2009). Our investigations reveal that Vasa functions as an RNA clamp to coordinate the assembly of a piRNA Amplifier complex on transposon transcripts. Within this protected environment, ATP hydrolysis by Vasa promotes safe handover of sliced piRNA intermediates between ping-pong partners.

Our results allow us to propose a step-by-step biochemical model for the Ping-pong cycle operating in BmN4 cells (Figure 7). Transposon silencing is initiated by cytoplasmic scanning of transposon transcripts by antisense primary piRNAs loaded into Siwi. This is closely followed by deposition of Vasa on the transcript and by assembly of the Amplifier by the joining of Qin/Kumo and Ago3 within the nuage. Amplifier assembly is linked to a conformational change in the core helicase domain of Vasa as it transitions from an ATP-unbound open state to the ATP- and RNA-bound closed state, such that the latter provides an interaction platform for the different components. Interestingly, Qin is already reported to facilitate heterotypic ping-pong between Aub (Siwi ortholog in *Drosophila*) and Ago3 by promoting interactions between them in the fly germline (Anand and Kai, 2012; Zhang et al., 2011). Siwi initiates the ping-pong cycle by slicing the target RNA to generate two fragments. Following this, the cleavage fragment carrying the mature 5′ end of a future secondary piRNA (piRNA intermediate) is transferred from Siwi to Ago3. We show that ATP hydrolysis by Vasa is critical for triggering this exchange and subsequent disassembly of the complex. We propose that the role of Vasa in assembling Amplifier is to generate a protective environment in which the ping-pong partners are brought to physical proximity, such that the cleaved target is not accessible to nucleases and is instead loaded onto Ago3 upon release from Siwi. Once acquired by Ago3, the mature 3′ end of the new piRNA is generated by an unknown 3′–5′ exonuclease, tentatively called Trimmer (Kawaoka et al., 2011). Such sense-oriented secondary piRNAs then guide Ago3 to participate in the feedforward step of the ping-pong cycle (Brennecke et al., 2007).

Our results provide, for the first time, a biochemical snapshot of events that take place during the ping-pong cycle. However, a number of questions still remain. It is not clear how the closed conformation of Vasa's helicase core domain can promote Amplifier assembly. In this context, it is tempting to draw a parallel between Vasa's role and the function of the helicase domain of the related DEAD box helicase eIF4AIII in nucleating the formation of the exon junction complex (EJC) on spliced mRNAs (Le Hir et al., 2000). In its ATP-bound closed conformation, the eIF4AIII core domain clamps on spliced mRNAs to provide a binding surface for other EJC components Mago, Y14, and Barentsz (Andersen et al., 2006; Bono et al., 2006). A similar situation can be envisaged during Amplifier assembly. Also unknown is whether any control is exercised over Siwi slicer activity to prevent futile cleavages that do not result in secondary piRNA production. Because piRNA intermediate exchange and complex disassembly are linked to ATP hydrolysis by Vasa, this might also be subject to regulation. It is only logical that target slicing by Siwi is followed by ATP hydrolysis by Vasa. We can only speculate that perhaps allosteric interactions between Piwi proteins and Vasa might link slicing of the target to ATP hydrolysis in Vasa. Recent genome-wide genetic screens have identified a number of factors that are implicated in the germline piRNA pathway in flies (Czech et al., 2013). An examination of our top hits in the Vasa^{DQAD} proteomics analyses (Figure S2A) did not reveal any overlaps except for the ping-pong Piwi partners and Qin/Kumo, which we validated in our study.

The ping-pong model predicts a reciprocal relationship in which piRNA-guided Siwi facilitates biogenesis of Ago3-bound piRNAs and vice versa (Brennecke et al., 2007). This means that there are potentially two distinct complexes mediating piRNA amplification: one occupying the Siwi-to-Ago3 segment and another one mediating the Ago3-to-Siwi feedforward step of the amplification loop. Our data strongly support a role for Vasa in the former step of the ping-pong cycle, but we cannot entirely rule out its participation in the latter. It is also possible that such a role in the feedforward segment might be fulfilled by other RNA helicases like Spn-E, a factor that is essential for the ping-pong cycle in flies (Malone et al., 2009), but not in mice (Shoji et al., 2009), wherein a linear secondary piRNA biogenesis pathway operates (De Fazio et al., 2011).

The DEAD box family is the largest family of helicases, and they are found from bacteria to humans, with most of the 26 members in yeast being essential for viability (de la Cruz et al., 1999). The in vivo RNA targets and RNP complexes of most DEAD box helicases have not been identified due to their transient nature. Here, we used a DQAD mutation to trap dynamic in vivo associations of Vasa. Structures of several DEAD box helicases with bound ATP analogs and RNA are closely related, indicating that perhaps similar outcomes to those we describe here can be expected for other family members assembling dynamic complexes in various RNA processing pathways.

EXPERIMENTAL PROCEDURES

Clones and Constructs

For expression studies in BmN4 cells, the coding sequence for the full-length *Bombyx mori* Vasa (GenBank accession number: NM_001043882.1) or its deletion versions were cloned into the pBEMBL-HA (Xiol et al., 2012) or pBEMBL-Myc vectors. Point mutations in the BmVasa helicase domain were introduced by an overlap PCR strategy: ATP-binding mutant (K230N; GKT→GNT) or ATP hydrolysis product-trap mutant (E339Q; DEAD→DQAD). The R→K mutant was created by converting 20 arginine (R) residues to lysines (K) at the Vasa N terminus (within a region spanning 1–117 aa) using a chemically synthesized DNA fragment. For live-cell imaging studies, the coding sequence for BmVasa, Vasa^{DQAD}, or Ago3 was cloned downstream of an enhanced green fluorescent protein (EGFP) tag or the red fluorescent protein variant mCherry in the pBEMBL vector backbone.

Crystallization and Biochemical Procedures

The helicase domain of *Bombyx* Vasa (135–564 aa) carrying the E339Q (DEAD→DQAD) mutation was produced in *E. coli* as a His-tagged fusion. Purified protein was incubated with a 6-mer (UGACAU) RNA and ATP or the ATP analog (AMPPNP) at a molar ratio of 1:1.2:1.2 (protein:RNA:ATP/AMPPNP). A summary of data collection statistics is provided in the Extended Experimental Procedures as Table S1.

Small RNA Sequencing

RNA libraries were prepared from immunoprecipitated complexes and were deep sequenced on the Illumina Hi-Seq (50 cycles) or MiSeq platforms (32 cycles). For long RNAs present in Vasa^{DQAD} complexes, a strand-specific RNA-seq library was prepared and sequenced on an Illumina Hi-Seq platform (105 cycles). Reads were aligned to the *Bombyx* genome and were analyzed using custom pipelines.

Fly Experiments

Drosophila vas mutant stocks were: *vas*^{PD} (Schupbach and Wieschaus, 1986) and *vas*^{D1} (Lehmann and Nüsslein-Volhard, 1991). The *vas*-deficient background was achieved by the use of the transheterozygotes (*vas*^{PD}/*vas*^{D1}). Expression of GFP-tagged *Drosophila melanogaster* Vasa transgenes (Johnstone and Lasko, 2004) in the fly germline was controlled from the upstream activating sequence (UAS) using GAL4 driven from a *nanos* promoter.

ACCESSION NUMBERS

The PDB accession codes for crystal structures are 4D26 and 4D25. Deep-sequencing data are deposited with Gene Expression Omnibus (GEO) (GSE57420).

SUPPLEMENTAL INFORMATION

Supplemental Information includes Extended Experimental Procedures, six figures, five movies, and two tables and can be found with this article online at http://dx.doi.org/10.1016/j.cell.2014.05.018.

ACKNOWLEDGMENTS

We thank Paul Lasko, Hugo Bellen, and Beat Suter for fly stocks/reagents. We are grateful to Sanjay Ghosh, Andrea Picco, Enrico Zamattia, Sandra Müller, and Anna Cyrklaff for help with data analysis and experiments. We thank the following EMBL core facilities: Advanced Light Microscopy, Genomics, Protein Expression and Purification, and High-Throughput Crystallization. Crystallographic data collection was at European Synchrotron Radiation Facility (ESRF), Grenoble, France. This work was supported by grants from European Union (European Research Council; "pisilence") to R.S.P. We are grateful for fellowships from the EMBL Interdisciplinary Postdoc Programme (EIPOD) under Marie Curie COFUND Actions (M.A.L), EMBO (D.H), and Region Rhone Alp (E.C.). This work was supported by the EMBL.

Received: February 25, 2014
Revised: April 28, 2014
Accepted: May 15, 2014
Published: June 5, 2014

REFERENCES

Anand, A., and Kai, T. (2012). The tudor domain protein kumo is required to assemble the nuage and to generate germline piRNAs in Drosophila. EMBO J. *31*, 870–882.

Andersen, C.B., Ballut, L., Johansen, J.S., Chamieh, H., Nielsen, K.H., Oliveira, C.L., Pedersen, J.S., Séraphin, B., Le Hir, H., and Andersen, G.R. (2006). Structure of the exon junction core complex with a trapped DEAD-box ATPase bound to RNA. Science *313*, 1968–1972.

Aravin, A.A., Hannon, G.J., and Brennecke, J. (2007). The Piwi-piRNA pathway provides an adaptive defense in the transposon arms race. Science *318*, 761–764.

Bagijn, M.P., Goldstein, L.D., Sapetschnig, A., Weick, E.M., Bouasker, S., Lehrbach, N.J., Simard, M.J., and Miska, E.A. (2012). Function, targets, and evolution of Caenorhabditis elegans piRNAs. Science *337*, 574–578.

Bono, F., Ebert, J., Lorentzen, E., and Conti, E. (2006). The crystal structure of the exon junction complex reveals how it maintains a stable grip on mRNA. Cell *126*, 713–725.

Brennecke, J., Aravin, A.A., Stark, A., Dus, M., Kellis, M., Sachidanandam, R., and Hannon, G.J. (2007). Discrete small RNA-generating loci as master regulators of transposon activity in Drosophila. Cell *128*, 1089–1103.

Brennecke, J., Malone, C.D., Aravin, A.A., Sachidanandam, R., Stark, A., and Hannon, G.J. (2008). An epigenetic role for maternally inherited piRNAs in transposon silencing. Science *322*, 1387–1392.

Caruthers, J.M., and McKay, D.B. (2002). Helicase structure and mechanism. Curr. Opin. Struct. Biol. *12*, 123–133.

Chen, Y., Pane, A., and Schüpbach, T. (2007). Cutoff and aubergine mutations result in retrotransposon upregulation and checkpoint activation in Drosophila. Curr. Biol. *17*, 637–642.

Czech, B., Preall, J.B., McGinn, J., and Hannon, G.J. (2013). A transcriptome-wide RNAi screen in the Drosophila ovary reveals factors of the germline piRNA pathway. Mol. Cell *50*, 749–761.

De Fazio, S., Bartonicek, N., Di Giacomo, M., Abreu-Goodger, C., Sankar, A., Funaya, C., Antony, C., Moreira, P.N., Enright, A.J., and O'Carroll, D. (2011). The endonuclease activity of Mili fuels piRNA amplification that silences LINE1 elements. Nature *480*, 259–263.

de la Cruz, J., Kressler, D., and Linder, P. (1999). Unwinding RNA in Saccharomyces cerevisiae: DEAD-box proteins and related families. Trends Biochem. Sci. *24*, 192–198.

de Vanssay, A., Bouge, A.L., Boivin, A., Hermant, C., Teysset, L., Delmarre, V., Antoniewski, C., and Ronsseray, S. (2012). Paramutation in *Drosophila* linked to emergence of a piRNA-producing locus. Nature *490*, 112–115.

Ghildiyal, M., and Zamore, P.D. (2009). Small silencing RNAs: an expanding universe. Nat. Rev. Genet. *10*, 94–108.

Grentzinger, T., Armenise, C., Brun, C., Mugat, B., Serrano, V., Pelisson, A., and Chambeyron, S. (2012). piRNA-mediated transgenerational inheritance of an acquired trait. Genome Res. *22*, 1877–1888.

Gunawardane, L.S., Saito, K., Nishida, K.M., Miyoshi, K., Kawamura, Y., Nagami, T., Siomi, H., and Siomi, M.C. (2007). A slicer-mediated mechanism for repeat-associated siRNA 5′ end formation in Drosophila. Science *315*, 1587–1590.

Johnstone, O., and Lasko, P. (2004). Interaction with eIF5B is essential for Vasa function during development. Development *131*, 4167–4178.

Kawaoka, S., Hayashi, N., Suzuki, Y., Abe, H., Sugano, S., Tomari, Y., Shimada, T., and Katsuma, S. (2009). The Bombyx ovary-derived cell line endogenously expresses PIWI/PIWI-interacting RNA complexes. RNA *15*, 1258–1264.

Kawaoka, S., Izumi, N., Katsuma, S., and Tomari, Y. (2011). 3′ end formation of PIWI-interacting RNAs in vitro. Mol. Cell *43*, 1015–1022.

Kawaoka, S., Hara, K., Shoji, K., Kobayashi, M., Shimada, T., Sugano, S., Tomari, Y., Suzuki, Y., and Katsuma, S. (2013). The comprehensive epigenome map of piRNA clusters. Nucleic Acids Res. *41*, 1581–1590.

Kazazian, H.H., Jr. (2004). Mobile elements: drivers of genome evolution. Science *303*, 1626–1632.

Kirino, Y., Vourekas, A., Kim, N., de Lima Alves, F., Rappsilber, J., Klein, P.S., Jongens, T.A., and Mourelatos, Z. (2010). Arginine methylation of vasa protein is conserved across phyla. J. Biol. Chem. *285*, 8148–8154.

Klattenhoff, C., Xi, H., Li, C., Lee, S., Xu, J., Khurana, J.S., Zhang, F., Schultz, N., Koppetsch, B.S., Nowosielska, A., et al. (2009). The Drosophila HP1 homolog Rhino is required for transposon silencing and piRNA production by dual-strand clusters. Cell *138*, 1137–1149.

Kuramochi-Miyagawa, S., Watanabe, T., Gotoh, K., Takamatsu, K., Chuma, S., Kojima-Kita, K., Shiromoto, Y., Asada, N., Toyoda, A., Fujiyama, A., et al. (2010). MVH in piRNA processing and gene silencing of retrotransposons. Genes Dev. *24*, 887–892.

Lasko, P.F., and Ashburner, M. (1988). The product of the Drosophila gene vasa is very similar to eukaryotic initiation factor-4A. Nature *335*, 611–617.

Le Hir, H., Izaurralde, E., Maquat, L.E., and Moore, M.J. (2000). The spliceosome deposits multiple proteins 20-24 nucleotides upstream of mRNA exon-exon junctions. EMBO J. *19*, 6860–6869.

Lehmann, R., and Nüsslein-Volhard, C. (1991). The maternal gene nanos has a central role in posterior pattern formation of the *Drosophila* embryo. Development *112*, 679–691.

Li, C., Vagin, V.V., Lee, S., Xu, J., Ma, S., Xi, H., Seitz, H., Horwich, M.D., Syrzycka, M., Honda, B.M., et al. (2009). Collapse of germline piRNAs in the absence of Argonaute3 reveals somatic piRNAs in flies. Cell *137*, 509–521.

Liang, L., Diehl-Jones, W., and Lasko, P. (1994). Localization of vasa protein to the Drosophila pole plasm is independent of its RNA-binding and helicase activities. Development *120*, 1201–1211.

Lim, A.K., and Kai, T. (2007). Unique germ-line organelle, nuage, functions to repress selfish genetic elements in Drosophila melanogaster. Proc. Natl. Acad. Sci. USA *104*, 6714–6719.

Linder, P., and Jankowsky, E. (2011). From unwinding to clamping - the DEAD box RNA helicase family. Nat. Rev. Mol. Cell Biol. *12*, 505–516.

Liu, F., Putnam, A., and Jankowsky, E. (2008). ATP hydrolysis is required for DEAD-box protein recycling but not for duplex unwinding. Proc. Natl. Acad. Sci. USA *105*, 20209–20214.

Luteijn, M.J., and Ketting, R.F. (2013). PIWI-interacting RNAs: from generation to transgenerational epigenetics. Nat. Rev. Genet. *14*, 523–534.

Malone, C.D., Brennecke, J., Dus, M., Stark, A., McCombie, W.R., Sachidanandam, R., and Hannon, G.J. (2009). Specialized piRNA pathways act in germline and somatic tissues of the Drosophila ovary. Cell *137*, 522–535.

Mathioudakis, N., Palencia, A., Kadlec, J., Round, A., Tripsianes, K., Sattler, M., Pillai, R.S., and Cusack, S. (2012). The multiple Tudor domain-containing protein TDRD1 is a molecular scaffold for mouse Piwi proteins and piRNA biogenesis factors. RNA *18*, 2056–2072.

Meister, G. (2013). Argonaute proteins: functional insights and emerging roles. Nat. Rev. Genet. *14*, 447–459.

Pane, A., Wehr, K., and Schüpbach, T. (2007). zucchini and squash encode two putative nucleases required for rasiRNA production in the Drosophila germline. Dev. Cell *12*, 851–862.

Pause, A., and Sonenberg, N. (1992). Mutational analysis of a DEAD box RNA helicase: the mammalian translation initiation factor eIF-4A. EMBO J. *11*, 2643–2654.

Schupbach, T., and Wieschaus, E. (1986). Germline autonomy of maternal-effect mutations altering the embryonic body pattern of Drosophila. Dev. Biol. *113*, 443–448.

Sengoku, T., Nureki, O., Nakamura, A., Kobayashi, S., and Yokoyama, S. (2006). Structural basis for RNA unwinding by the DEAD-box protein Drosophila Vasa. Cell *125*, 287–300.

Shoji, M., Tanaka, T., Hosokawa, M., Reuter, M., Stark, A., Kato, Y., Kondoh, G., Okawa, K., Chujo, T., Suzuki, T., et al. (2009). The TDRD9-MIWI2 complex is essential for piRNA-mediated retrotransposon silencing in the mouse male germline. Dev. Cell *17*, 775–787.

Xiol, J., Cora, E., Koglgruber, R., Chuma, S., Subramanian, S., Hosokawa, M., Reuter, M., Yang, Z., Berninger, P., Palencia, A., et al. (2012). A role for Fkbp6 and the chaperone machinery in piRNA amplification and transposon silencing. Mol. Cell *47*, 970–979.

Zhang, Z., Xu, J., Koppetsch, B.S., Wang, J., Tipping, C., Ma, S., Weng, Z., Theurkauf, W.E., and Zamore, P.D. (2011). Heterotypic piRNA Ping-Pong requires qin, a protein with both E3 ligase and Tudor domains. Mol. Cell *44*, 572–584.

Zhang, F., Wang, J., Xu, J., Zhang, Z., Koppetsch, B.S., Schultz, N., Vreven, T., Meignin, C., Davis, I., Zamore, P.D., et al. (2012). UAP56 couples piRNA clusters to the perinuclear transposon silencing machinery. Cell *151*, 871–884.